Publications of the Astronomical Society of Australia (PASA), Vol. 32, e023, 11 pages (2015).

doi:10.1017/pasa.2015.23

Light Curve Solutions of Ten Eccentric *Kepler* Binaries, Three of them with Tidally Induced Humps

D. Kjurkchieva[1] and D. Vasileva*

Department of Physics, Shumen University, 9700 Shumen, Bulgaria
[1]Email: d.kyurkchieva@shu-bg.net

(Received March 8, 2015; Accepted May 4, 2015)

Abstract

We carried out light curve solutions of ten detached eclipsing eccentric binaries observed by *Kepler*. The formal errors of the derived parameters from the light curve solutions are below 1%. Our results give indications that the components of the eccentric binaries (especially those with mass ratios below 0.5) do not follow precisely the empirical relations between the stellar parameters derived from the study of circular-orbit binaries. We found the following peculiarities of the targets: (a) the components of KIC 9474969 have almost the same temperatures while their radii and masses differ by a factor around 2.5; (b) KIC 6949550 reveals semi-regular light variations with an amplitude of 0.004 and a period around 7 d which are modulated by long-term variations; (c) KIC 6220470, KIC 11071207, and KIC 9474969 exhibit tidally induced 'hump' around the periastron. These are the targets with the biggest relative radii of our sample. We derived the dependence of the hump amplitude on the relative stellar radii, eccentricity, and mass ratio of eccentric binary consisting of MS stars.

Keywords: binaries: eclipsing – stars: fundamental parameters – stars: individual: KIC 6220470, KIC 8296467, KIC 6877673, KIC 9658118, KIC 12306808, KIC 5553624, KIC 9474969, KIC 11391181, KIC 11071207, KIC 6949550

1 INTRODUCTION

The majority of studies on binaries have focused on near-circular orbits (Pichardo et al. 2005). However, it is generally supposed that eccentric binaries are mainly produced as a result from the fragmentation (Bonnell & Bastien 1992; Bate 1997; Bate & Bonnell 1997). Moreover, the empirical data reveal that the main-sequence binary systems typically have eccentric orbits (Duquennoy & Mayor 1991). The probable reason the eccentric binaries to be poorly studied is that they are wide stellar systems with long periods (Bate, Bonnell, & Bromm 2002) requiring prolonged observations. Recently, this condition was satisfied by huge surveys such as the Robotic Optical Transient Search Experiment (ROTSE), Massive Compact Halo Objects (MACHO), All Sky Automated Survey (ASAS), SuperWASP, etc. The next important step was made by the space mission *Kepler* (Koch et al. 2010). Due to its extended and nearly uninterrupted data set above thousand detached systems were discovered, considerable parts of them on eccentric orbits.

Kepler not only provided many new eccentric binaries but the unique precision of its observational data transformed these binary stars from objects of the celestial mechanics to an important field of the stellar astrophysics. They became probes for study of the tidal phenomena: mechanisms for circularisation of the orbits and synchronisation of the stellar rotation with the orbital motion; impermanent mass transfer occurring close to the periastron (Sepinsky, Willems, & Kalogera 2007a; Lajoie & Sills 2011); apsidal motion; tidally excited brightening and oscillations.

The theoretical studies reveal that the secular changes of the orbital separation and eccentricity could be positive or negative (depending on the mass ratio and eccentricity), and could occur on timescales ranging from a few million years to a few billion years (Sepinsky et al. 2007b, 2009). Thus, the widespread assumption for rapid circularisation becomes inapplicable, i.e., binaries can remain on eccentric orbits for long periods of time. Hence, the binary stars on eccentric orbits have an important evolutional role.

The eclipsing eccentric binaries (EEBs) with an apsidal motion provide an important observational test of the theoretical models of stellar structure and evolution (Kopal 1978; Claret & Gimenez 1993). The coefficients of internal structure k_j are used to describe the external potential of a distorted configuration as a function of its internal structure in the form

*database of the *Kepler* mission

of series expansion (Claret & Gimenez 1991). In most cases, only k_2 is important since higher harmonics in the apsidal motion decrease rapidly. In order to compare with observations, an average value $\bar{k}_2 = (c_1 k_{12} + c_2 k_{22})/(c_1 + c_2)$ of the contribution of star 1 and 2 (k_{12} and k_{22}) is used. The coefficients c_1 and c_2 are known functions of observable stellar and orbital parameters (eccentricity, radii, masses, and rotational velocities). The individual contributions can be separated in two terms, rotational and tidal. In most cases, tidal terms dominate the apsidal motions of binary systems (Claret & Gimenez 1993). Hence, the 'apsidal motion test' could be used as a probe of stellar internal structure if precise values of global parameters are available (Claret & Gimenez 2010). There are important recent studies of this effect based on the observed apsidal motion of double-lined binaries (Lacy et al. 2015; Zasche et al. 2014; Bulut, Bulut, & Cicek 2014; Garcia et al. 2014; Kozyreva & Kusakin 2014; Harmanec et al. 2014; Wilson & Van Hamme 2014; Hambleton et al. 2013; Wolf et al. 2013; Claret 2012; Zasche 2012; Kuznetsov et al. 2011; Claret & Gimenez 2010; Wolf et al. 2010; Gimenez & Quintana 1992; Barembaum & Etzel 1995; etc.) .

In addition to the classical Newtonian contribution, the observed apsidal motion includes term of the General Relativity (Levi-Civita 1937; Gimenez 1985). Information for the apsidal motions of 128 targets in our Galaxy can be found in the catalogue of Petrova & Orlov (1999). The study of EEBs in close galaxies SMC and LMC began in the new millenium (Graczyk 2003; Michalska & Pigulski 2005; Michalska 2007; Bulut & Demircan 2007; North et al. 2010; Zasche & Wolf 2013; Zasche et al. 2014).

Probably the most amazing peculiarities of the binary stars on eccentric orbits are the tidally excited oscillations (harmonics of the orbital period) and brightening around the periastron. They were theoretically predicted by Kumar, Ao, & Quataert (1995) to explain the ~1 d oscillations with amplitude of 0.002 of *B*-type star orbiting a neutron star (radio pulsar PSR 0045–7319 with $e = 0.81$ and $P_{orb} = 51$ d). Further, this analytic theory was used for the explanation of (a) the oscillation with frequency of exactly ten times the orbital frequency of the slowly pulsating *B*-star in the binary HD177863 (De Cat et al. 2000); (b) the oscillations of the *A*-type primary of the eccentric binary HD 209295 (Handler et al. 2002); and (c) the oscillations of the eccentric, short-period early-type binary HD 174884 (Maceroni et al. 2009).

The theory of the tidally excited phenomena further was developed by Willems (2003), Zahn (2005), Willems & Claret (2005), Willems (2007), Hernandez-Gomez et al. (2011), Gundlach & Murphy (2011), Burkart et al. (2012), Song et al. (2013), Borkovits et al. (2014), etc.

Brilliant confirmations of the theoretical predictions of Kumar et al. (1995) were discovered by the *Kepler* mission. KOI 54 exhibits two remarkable features – a periodic brightening spike of 0.7% occurring at the periastron and a 0.1% 'beat' pattern of pulsations in phase with the brightening events (Welsh et al. 2011, Burkart et al. 2012). Thompson et al. (2012) discovered the next 16 similar objects (most of them non-eclipsing) in the *Kepler* archive and called them 'heartbeat' stars due to their shape of light variability reminiscent of an echocardiogram. Their light curves are different–some dim before they brighten, others dim after they brighten, and others show distinct W or M shapes. Stellar oscillations at harmonics of the heartbeat periods of some of these targets were also found.

Answering to the appeal to use the available resources of the *Kepler* database for additional research, we undertook study of some types of binary systems from the eclipsing binary (EB) catalogue (Dimitrov, Kjurkchieva, & Radeva 2012; Kjurkchieva & Dimitrov 2015). The goal of this study was to obtain the orbits and parameters of ten eccentric binaries based on the *Kepler* data as well as to search for tidally induced phenomena.

2 SELECTION OF THE TARGETS

Above two thousand EBs have been identified and included in the *Kepler* EB catalogue (Prsa et al. 2011; Slawson et al. 2011); around 1 261 of them have been initially classified as detached systems. An automate fitting of the light curves have been used for determination of their ephemerides.

We reviewed visually the *Kepler* EB catalogue to search for detached binaries with eccentric orbits and found around 250 targets in which phase difference between the primary and secondary minimum differed considerably from 0.5 and in which durations of the two light minima were not equal. Most of the found light curves were with quite narrow eclipses (due to the long periods). We chose to model ten binaries with relatively long eclipses (above 0.01 in phase units) allowing precise light curve solutions.

Table 1 presents available information for the targets (Prsa et al. 2011): orbital period *P*; *Kepler* magnitude *kmag*; mean temperature T_m; width of the primary eclipse w_1 (in phase units); width of the secondary eclipse w_2 (in phase units); depth of the primary eclipse d_1 (in flux units); depth of the secondary eclipse d_2 (in flux units). We added to the available target data in Table 1 the phases φ_2 of their secondary eclipses (the phases φ_1 of the primary eclipses are 0.0).

The detailed review of the *Kepler* data of our targets revealed that their light curves did not change during the different cycles and observational quarters. This allows for modelling to any data set. We chose to use several consecutive cycles from the middle quarters of each target.

3 LIGHT CURVE SOLUTIONS

We carried out the modelling of the *Kepler* data by the binary modelling package PHOEBE (Prsa & Zwitter 2005) . It is based on the Wilson–Devinney (WD) code (Wilson & Devinney 1971; Wilson 1979; Wilson & Van Hamme 2004). PHOEBE incorporates all the functionality of the WD code but also provides a graphical user interface alongside other improvements, including updated filters for the various recent space missions as *Kepler*. That is why PHOEBE is highly

Table 1. Parameters of the targets from the EB catalogue (period P, *Kepler* magnitude *kmag*, mean temperature T_m, widths w_i, and depths d_i of the eclipses) and phases of the secondary eclipses φ_2.

Star	P [d]	*kmag*	T_m	w_1	w_2	d_1	d_2	φ_2
KIC 6220470	8.144 136	13.960	7377	0.045	0.037	0.091	0.010	0.400
KIC 8296467	10.333 56	15.177	5316	0.024	0.016	0.531	0.326	0.625
KIC 6877673	36.758 887	13.676	5819	0.016	0.013	0.273	0.188	0.439
KIC 9658118	24.059 995	14.158	6225	0.017	0.035	0.473	0.457	0.603
KIC 12306808	37.878 484	13.265	5738	0.011	0.013	0.220	0.169	0.555
KIC 5553624	25.762 071	14.231	5358	0.023	0.007	0.449	0.246	0.420
KIC 9474969	21.570 506	12.462	6085	0.027	0.023	0.133	0.116	0.759
KIC 11391181	8.617 340	15.257	5218	0.017	0.019	0.181	0.106	0.607
KIC 11071207	8.049 635	13.831	6427	0.031	0.040	0.279	0.140	0.621
KIC 6949550	7.841 067	15.144	5719	0.033	0.031	0.355	0.350	0.332

appropriate for modelling of the precise *Kepler* data (Hambleton et al. 2013).

We used several considerations for the light curve solutions.

(1) The almost flat out-of-eclipse parts of the observed light curve gave us the grounds to use the detached mode of modelling.

(2) The light curve solution of eccentric binaries by PHOEBE (also by each light curve synthesis software) without any guessed values of the eccentricity e and periastron angle ω is quite time-consuming task. That is why we calculated preliminary values of these orbit parameters by the formulae

$$e_0 \cos\omega_0 = \frac{\pi}{2}[(\varphi_2 - \varphi_1) - 0.5] \qquad (1)$$

$$e_0 \sin\omega_0 = \frac{w_2 - w_1}{w_2 + w_1}. \qquad (2)$$

They were obtained as approximations of formulae (9–25) and (9–37) of Kopal (1978). We calculated e_0 and ω_0 by our expressions (1–2) using the values of φ_2, w_1 and w_2 from Table 1 ($\varphi_1 = 0$). The obtained values of e_0 and ω_0 were used as input parameters of PHOEBE.

(3) The mean temperatures T_m of our targets (Table 1) allowed us to adopt coefficients of gravity brightening 0.32 and reflection effect 0.5 appropriate for stars with convective envelopes. The only exception was the hot primary of KIC 6220470 requiring parameters of star with radiative envelope (gravity brightening 1.0 and reflection effect 1.0). The contribution of the gravity brightening effect (and its coefficients) is not considerable for detached binaries as our targets.

(4) Initially the synchronicity parameters were kept fixed at values of unity.

(5) Initially the primary temperature T_1 was fixed to be equal to the mean target temperature T_m (Table 1) that has been estimated using dedicated pre-launch ground-based optical multi-colour photometry plus Two Micron All Sky Survey (2MASS) J, K, and H magnitudes (Prsa et al. 2011).

Table 2. The derived orbital parameters of the targets: eccentricity e, periastron angle ω, and periastron phase $\varphi_{\text{per.}}$

Star	e	ω [deg]	φ_{per}
KIC 6220470	0.1879 ± 0.0002	215.03 ± 0.01	0.294
KIC 8296467	0.2781 ± 0.0001	314.48 ± 0.01	0.696
KIC 6877673	0.1704 ± 0.0002	235.26 ± 0.01	0.369
KIC 9658118	0.3723 ± 0.0001	66.01 ± 0.01	0.971
KIC 12306808	0.1089 ± 0.0001	36.74 ± 0.01	0.878
KIC 5553624	0.5204 ± 0.0001	258.12 ± 0.01	0.411
KIC 9474969	0.4165 ± 0.0001	354.78 ± 0.01	0.867
KIC 11391181	0.1797 ± 0.0001	18.94 ± 0.01	0.854
KIC 11071207	0.2256 ± 0.0004	33.00 ± 0.01	0.897
KIC 6949550	0.2661 ± 0.0001	186.64 ± 0.01	0.183

Our procedure of the light curve solutions was quite similar to that of Hambleton et al. (2013) and was carried out in several stages.

At the very beginning, we input some guessed values of the secondary temperature T_2, mass ratio q, orbital inclination i, and potentials $\Omega_{1,2}$ and varied only the eccentricity e and periastron angle ω around their input values e_0 and ω_0 to search for the best fit of the phases of the eclipses estimated by the value of χ^2. It turned out that the final values e and ω differed from the input values up to 10%. This means that the approximated formulae (1–2) could be used successfully for calculation of the input values of eccentricity and periastron angle of eccentric binaries.

At the second stage, we fixed e and ω and varied simultaneously T_2, q, i, and $\Omega_{1,2}$ (and thus relative radii $r_{1,2}$). We used linear limb-darkening law with limb-darkening coefficients corresponding to the stellar temperatures and *Kepler* photometric system (Claret & Bloemen 2011).

Finally, to adjust the stellar temperatures T_1 and T_2 around the mean value T_m, we used the procedure described in Dimitrov & Kjurkchieva (2015).

The final parameters of the eccentric orbits are given in Table 2, while Table 3 contains the parameters of the stellar configurations. The synthetic curves corresponding to the parameters of our light curve solutions are shown in Figures 1–10 as continuous lines.

Table 3. Parameters of the best light curve solutions: orbital inclination i, mass ratio q, temperatures T_i, relative radii r_i, and relative luminosities l_i of the stellar components.

Star	i	q	T_1 [K]	T_2 [K]	r_1	r_2	l_1	l_2/l_1
KIC 6220470	89.50	0.446	7875	4382	0.1014	0.0286	0.9918	0.0082
	±0.01	±0.001	±267	±70	±0.0010	±0.0005		
KIC 8296467	89.58	0.776	5726	5077	0.0344	0.0325	0.6478	0.5436
	±0.01	±0.001	±8	±6	±0.0003	±0.0004		
KIC 6877673	89.71	0.798	6117	5706	0.0312	0.0169	0.8234	0.2144
	±0.01	±0.004	±29	±25	±0.0010	±0.0010		
KIC 9658118	89.93	0.973	6212	6193	0.0431	0.0396	0.5445	0.8365
	±0.01	±0.002	±3	±3	±0.0002	±0.0001		
KIC 12306808	88.668	0.807	5772	5693	0.0249	0.0214	0.5910	0.6920
	±0.001	±0.001	±4	±3	±0.0001	±0.0004		
KIC 5553624	89.623	0.682	6122	5120	0.0244	0.0200	0.7772	0.2866
	±0.002	±0.001	±8	±5	±0.0003	±0.0005		
KIC 9474969	87.94	0.403	5737	5574	0.0679	0.0258	0.8876	0.1266
	±0.01	±0.002	±47	±45	±0.0001	±0.0050		
KIC 11391181	87.42	0.7728	5199	4778	0.04805	0.03125	0.7868	0.2709
	±0.01	±0.0014	±5	±4	±0.00030	±0.00010		
KIC 11071207	87.47	0.4304	6836	5913	0.0793	0.0446	0.8518	0.2861
	±0.01	±0.0020	±24	±19	±0.0007	±0.0013		
KIC 6949550	88.45	0.9859	5802	5784	0.0504	0.0502	0.5058	0.9770
	±0.01	±0.0018	±6	±5	±0.0008	±0.0007		

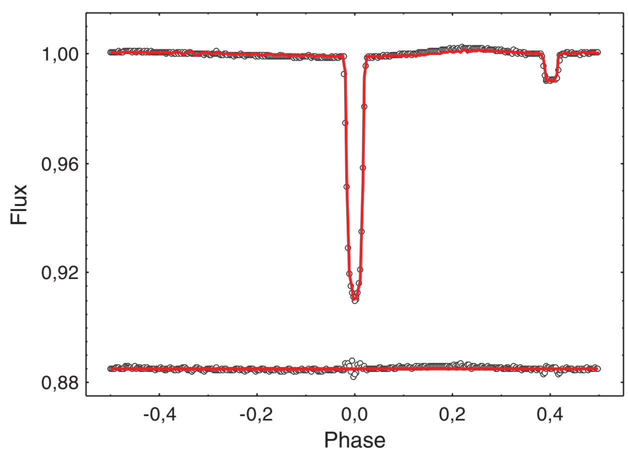

Figure 1. Top: the folded light curve of KIC 6220470 and its fit; Bottom: the corresponding residuals (shifted vertically by different number to save space). Colour version of this figure is available in the online journal.

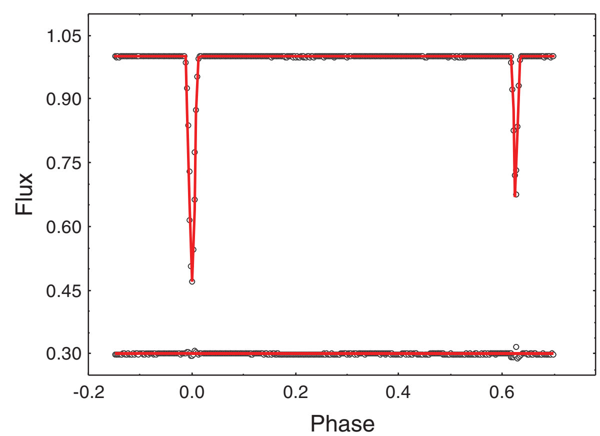

Figure 2. Same as Figure 1 for KIC 8296467.

Any surface spots and third lights were not necessary to reproduce the photometric data and thus, the condition the synchronicity parameters to be fixed at unity turned out without consequence.

The errors in Tables 2–3 are the formal PHOEBE errors. Most of them are smaller than 1%, excluding the temperatures of the stellar components of KIC 6220470 whose errors exceed 3%. We attributed these bigger errors to the considerably shallower eclipses of this target, especially the secondary one (see Table 1). The small errors of the derived parameters by our light curve solutions are natural consequence of the high precision of the *Kepler* data.

However, one can see two imperfections in the reproducing of the data.

The first one is the relative bigger residuals during the eclipses (Figures 1–10). Similar behaviour could be seen also for other *Kepler* binaries (Hambleton et al. 2013; Lehmann et al. 2013; Maceroni et al. 2014). We attributed them to the effects of finite integration time studied by Kipping (2010): (i) the large integration times smear out the light curve signal into a broader shape (see Figure 1 of Kipping 2010): the detected ingress and egress durations are bigger than their natural values (introducing an additional curvature into the eclipse wings) and the apparent positions of the contact points are temporally shifted from their true value; (ii) the large integration times smear out the curvature of the eclipse

Table 4. Masses M_i, **radii** R_i, **and luminosities** L_i **of the target components (in solar units) according to the empirical relations. Their errors are due to the interpolation process.**

Star	M_1	M_2	R_1	R_2	L_1	L_2
KIC 6220470	1.75 ± 0.09	0.80 ± 0.01	1.95 ± 0.08	0.73 ± 0.09	10.9 ± 2.2	0.18 ± 0.02
KIC 8296467	1.00 ± 0.01	0.88 ± 0.01	1.20 ± 0.01	1.04 ± 0.01	1.47 ± 0.01	0.52 ± 0.01
KIC 6877673	1.05 ± 0.01	0.95 ± 0.01	1.31 ± 0.01	1.19 ± 0.01	2.63 ± 0.09	1.41 ± 0.04
KIC 9658118	1.09 ± 0.01	1.08 ± 0.01	1.33 ± 0.01	1.32 ± 0.01	3.01 ± 0.01	3.01 ± 0.01
KIC 12306808	0.96 ± 0.01	0.95 ± 0.01	1.20 ± 0.01	1.18 ± 0.01	1.51 ± 0.01	1.38 ± 0.01
KIC 5553624	1.05 ± 0.01	0.86 ± 0.01	1.31 ± 0.01	1.05 ± 0.01	2.63 ± 0.02	0.56 ± 0.01
KIC 9474969	1.06 ± 0.02	0.94 ± 0.01	1.32 ± 0.01	1.16 ± 0.02	1.47 ± 0.09	1.14 ± 0.06
KIC 11391181	0.89 ± 0.01	0.85 ± 0.01	1.07 ± 0.01	0.92 ± 0.01	0.61 ± 0.01	0.32 ± 0.01
KIC 11071207	1.40 ± 0.01	0.98 ± 0.01	1.53 ± 0.01	1.24 ± 0.01	5.62 ± 0.11	1.90 ± 0.04
KIC 6949550	0.97 ± 0.01	0.96 ± 0.01	1.21 ± 0.01	1.21 ± 0.01	1.58 ± 0.01	1.51 ± 0.01

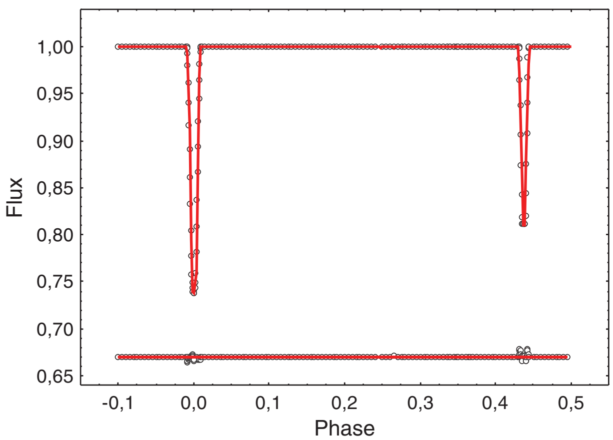

Figure 3. Same as Figure 1 for KIC 6877673.

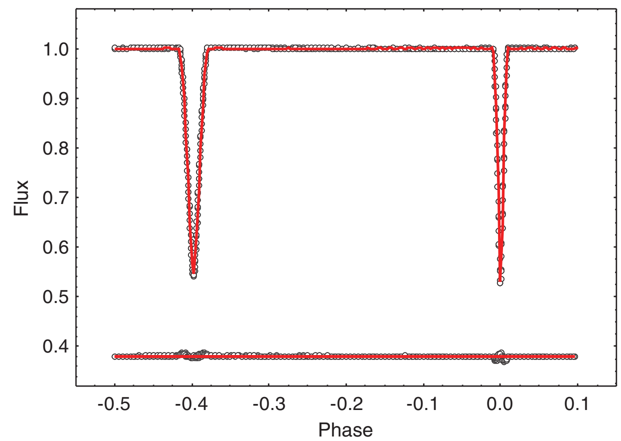

Figure 4. Same as Figure 1 for KIC 9658118.

bottom caused by the limb-darkening effect. The two effects are inherent to the long-cadence *Kepler* data of our targets used for modelling. Coughlin et al. (2011) also found that the long-cadence (integration time of 29.43 min) *Kepler* data of systems with small sum of relative radii significantly alter the morphological shape of a light curve.

The second imperfection is the small ripples on the flat out-of-eclipse sections of some synthetic light curves as well as those on the flat bottom of the total eclipses. We attributed them to numerical shortcoming of the software for the cases of binaries with small relative radii of the components. Such effect (with amplitude below 0.1 mmag) was firstly noted by Maceroni et al. (2009) and interpreted by the description of stellar surfaces with a finite number of elements. The result of the surface discretisation seems bigger (with amplitude around 0.2 mmag) for our targets in which components have small relative radii. In fact, this is the reason for the traditional software for light curve synthesis to be not applicable for modelling of exoplanet transits (see for instance PHOEBE *scientific reference* by Prsa et al. 2011).

We estimated the global parameters of the target components (Table 4) using the empirical statistical relations mass–temperature, radius–temperature, and luminosity–temperature for MS stars (Boyajian et al. 2013), which were approximated by combinations of linear functions. Thus, the absolute parameters in Table 4 are result of interpolation of empirical relations, not derived from observational data, and the listed errors are due to the interpolation process.

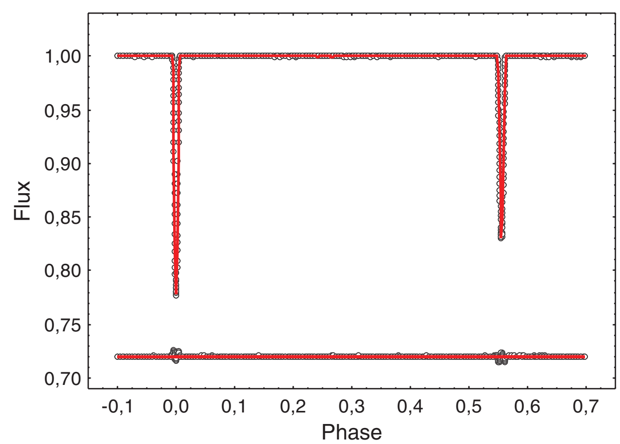

Figure 5. Same as Figure 1 for KIC 12306808.

doi:10.1017/pasa.2015.23

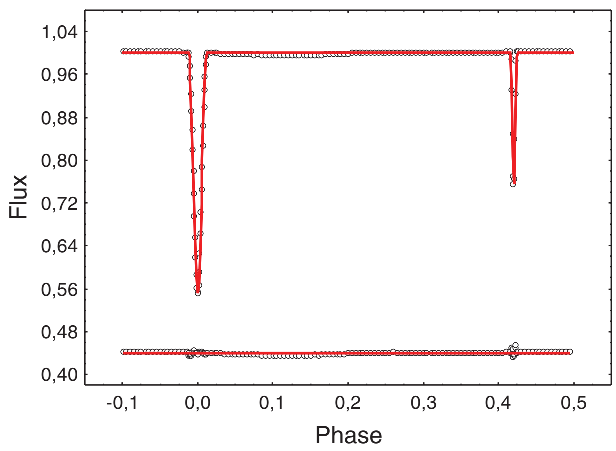

Figure 6. Same as Figure 1 for KIC 5553624.

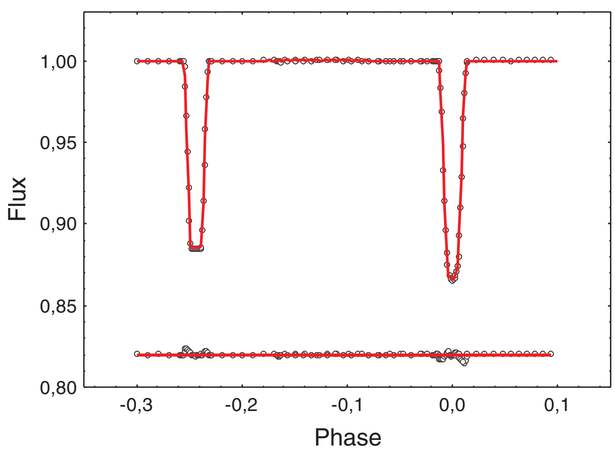

Figure 7. Same as Figure 1 for KIC 9474969.

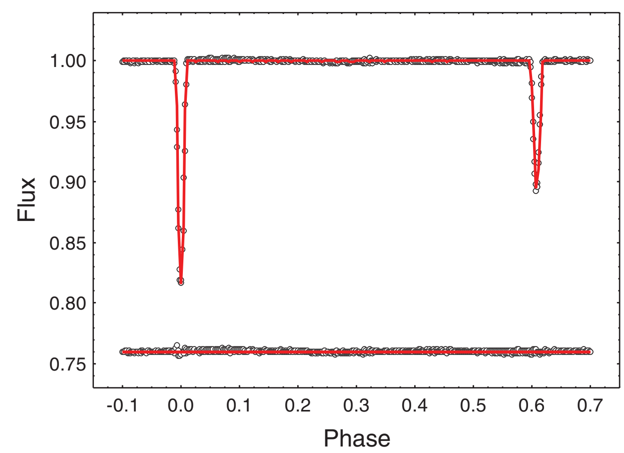

Figure 8. Same as Figure 1 for KIC 11391181.

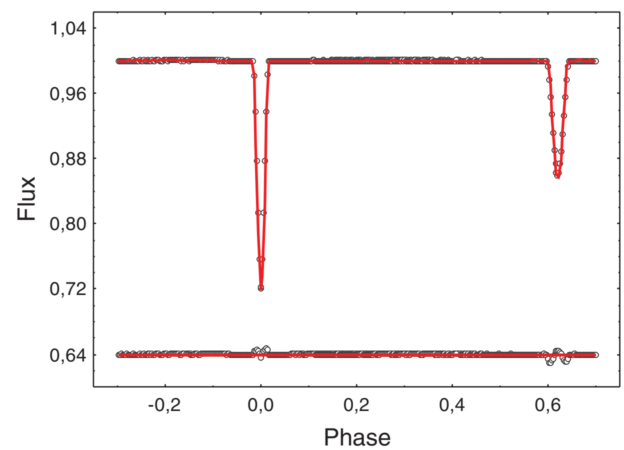

Figure 9. Same as Figure 1 for KIC 11071207.

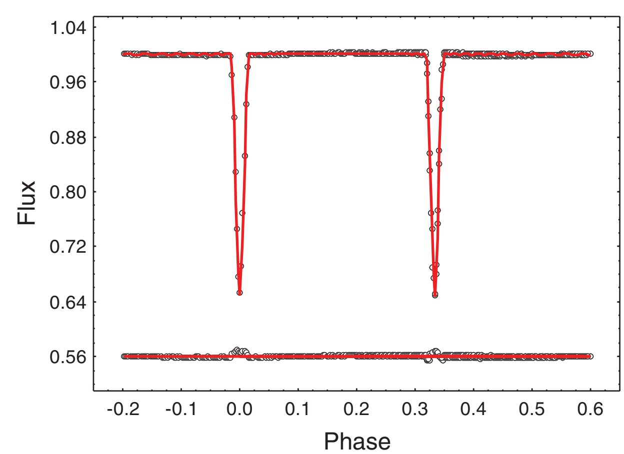

Figure 10. Same as Figure 1 for KIC 6949550.

4 DISCUSSION

The analysis of the light curve solutions of the chosen ten eccentric binaries led us to several important results.

(1) We established high sensibility of the solutions (measured by χ^2) to the mass ratio (Figure 11). This result differed from those of Michalska & Pigulski (2004) and Terrell & Wilson (2005) who found that for detached EBs equally good fits can be obtained in a very large range of mass ratios. We attributed the sensibility of our solutions to the mass ratio to the following: high precision of the *Kepler* data, very small relative radii of the stars of our sample, and eccentric orbits of our targets.

(2) The temperatures of the stellar components correspond to spectral type from late *A* to middle *K* with dominance of *G* type. This result is expected taking into account that *Kepler* observed mainly solar-type stars.

(3) Our targets have quite big eccentricities ($0.11 \leq e \leq 0.52$). This result is due to the selection effect and thus does not contradict to the expected distribution of e peaked at 0.0–0.1 (Prsa et al. 2008).

Our targets do not support the expected relation of the eccentricity to be smaller for the shorter period systems (the shorter period orbits undergo stronger tidal forces

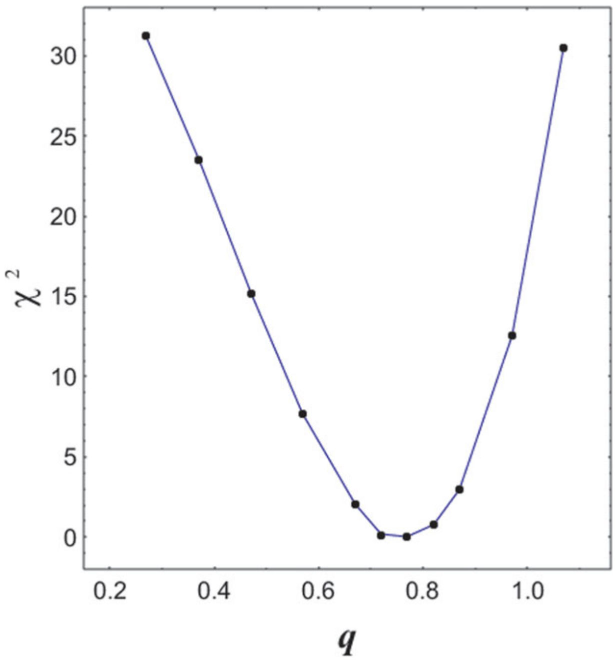

Figure 11. Sensibility of our light curve solution of KIC 11391181 (measured by χ^2) to the mass ratio (the rest parameters last fixed at their final values).

and they circularise more quickly, leaving a dearth of highly eccentric short period binaries). Such a trend of increasing of e with the period has been established for evolved MS stars in open cluster M67 (Mathieu & Mazeh 1988).

(4) The orbital inclinations of the targets are quite near to the 90° (Table 3) that is expected for eclipsing systems with periods above 8 d. But only two targets, KIC 6220470 and KIC 9474969, undergo total eclipses.

(5) We did not find evidence for apsidal motion of our targets. The possible reason is the relative short duration of the *Kepler* observations. Typically, apsidal periods are at least a decade long (Michalska & Pigulski 2005). Moreover, the systems with apsidal motions are with the shortest orbital periods or with the largest sum of relative radii for a given eccentricity (Michalska 2007), but these conditions are not fulfilled for our targets.

(6) The out-of-eclipse light of the targets is constant within 0.2%. Only KIC 6949550 consisting of two solar-type stars reveals semi-regular light variations (Figures 12 and 13) with amplitudes of 0.002–0.004 on timescales of order of 7 d (Figure 12) which are modulated with a period around 400 d (Figure 13). The possibility for these low-amplitude variations to be detected is due to the unprecedented precision of the *Kepler* data. Their frequency analysis is object of future study.

(7) The review of the light curves of our targets from different quarters did not exhibit any long-term variability (excluding KIC 6949550).

(8) The mass ratios of the targets are within the range 0.4–1.0. North et al. (2010) obtained that q for detached systems is within 0.8–1.1 and for semidetached and contact binaries within 0.4–0.7. Lucy (2006) found an excess of binary systems with $q \geq 0.95$ in our Galaxy. Our result implies that the distribution of the mass ratio for eccentric binaries differs from that for circular-orbit systems.

(9) We established some linear trend between the ratio r_2/r_1 and mass ratio q (Figure 14, left) for the ten members of our small sample.

(10) The ratios T_2/T_1 of our targets fall in the range 0.8–1.0 with one exception, KIC 6220470, which value is 0.56 (Figure 14, middle). Opposite discrepancy has been found for HD 174884 (Maceroni et al. 2009), which components are with equal temperatures irrespective of the negligible secondary eclipse.

(11) The values q_{st} of the mass ratios, obtained by the empirical relation temperature–mass of MS stars (Table 4), differed from those determined by our PHOEBE models $q \equiv q_{PH}$ (Figure 14, right). The most glaring case is KIC 9474969 with values $q_{st} = 0.88$ and $q_{PH} = 0.4$.

Figure 14 implies that the components of the eccentric binaries, especially those with $q \leq 0.5$, do not follow the empirical relations between the global stellar parameters derived by study of circular-orbit binaries (and with probable

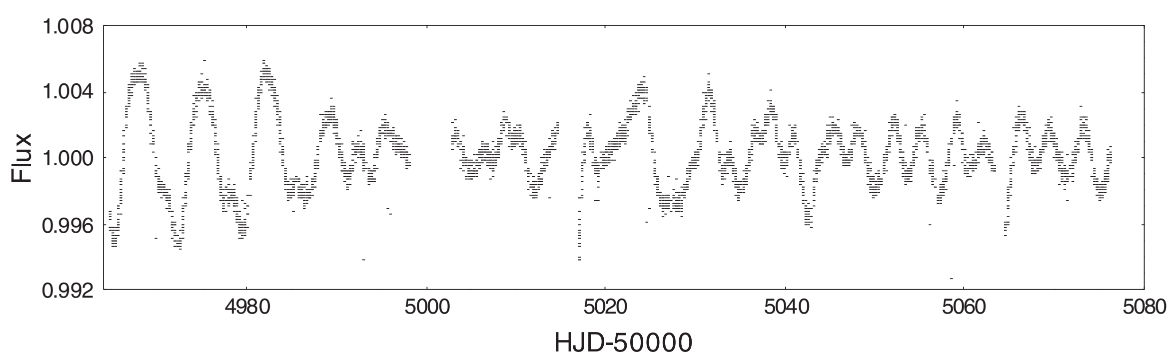

Figure 12. Short-term semi-regular light variations of KIC 6949550.

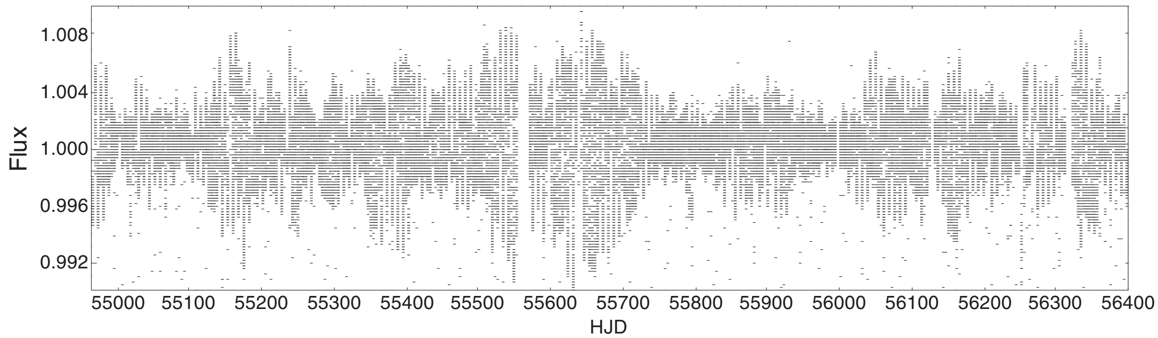

Figure 13. Long-term modulation of the light variations of KIC 6949550.

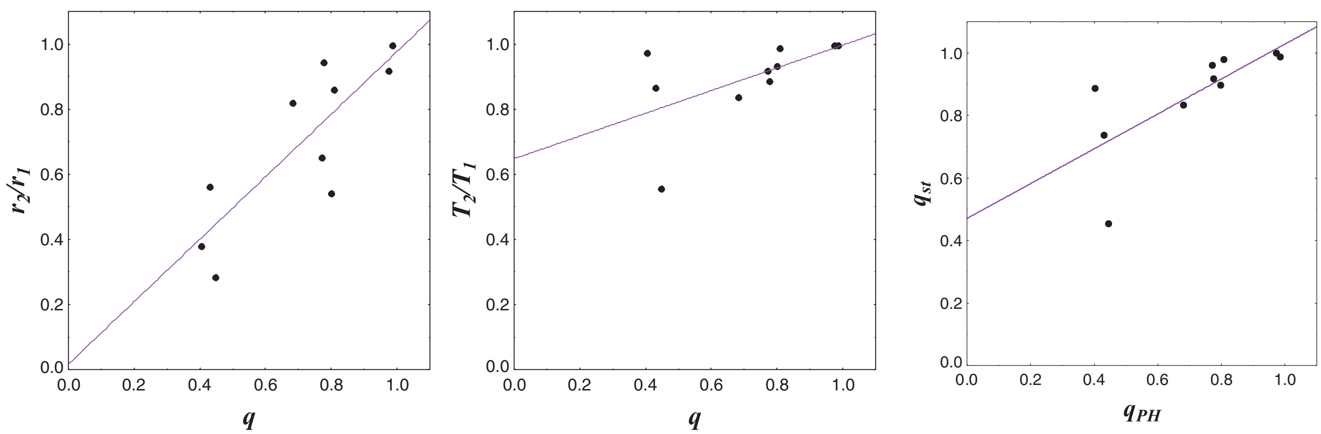

Figure 14. Dependence of r_2/r_1 on mass ratio q (left panel), dependence of T_2/T_1 on mass ratio q (middle panel), and diagram $q_{st} - q_{PH}$ (right panel).

dominance of mass ratios around unity). In fact, only targets KIC 9658118 and KIC 6949550 with mass ratio near unity turned out with almost equal values of the ratios of luminosities and radii of their components obtained by the light curve solutions (l_2/l_1 and r_2/r_1 from Table 2) and by the empirical relations for MS stars (L_2/L_1 and R_2/R_1 from Table 4). The biggest discrepancies between the values of these ratios belong to KIC 9474969 with the smallest mass ratio. This result might be considered as some empirical support of the conclusion of Sepinsky et al. (2007a) about the difference of the Roche geometry of circular-orbit and eccentric-orbit binaries. Another possible reason could be that the empirical relations for MS stars have been derived on the base of binaries with mass ratios around unity.

5 TIDALLY INDUCED HUMPS

The tidal forces change the stellar shape (tidal bulges) and cause brightness variability due to projection of the distorted stellar surfaces on the visible plane (Brown et al. 2011; Welsh et al. 2011; Morris 1985). It has double-wave shape (ellipsoidal variations) in the case of circular orbits and light increasing around the periastron in the case of eccentric orbits.

Kumar et al. (1995) created an analytic model of tidal phenomena in eccentric binary consisting of point source (neutron star) and MS star. The shape of the corresponding light curve depends on inclination, angle of periastron, and eccentricity while its amplitude (of order of mmag) depends on the masses of the objects, their internal stellar structure, and the orbital separation at the periastron (Kumar et al. 1995). According to this model, the shape of the light increase is one-peaked for $i \leq 30°$ but becomes two-peaked with central dip (which depth and width increase with i) for the bigger orbital inclination.

Thompson et al. (2012) calculated a grid of solutions to the model of Kumar et al. (1995) and found that the larger inclinations cause the light curve firstly to increase in brightness and then to decrease (KIC 3547874), or vice versa (KIC 9790355), depending on the angle of periastron, while the bigger eccentricity led to shorter duration of the heartbeat event.

Three targets from our sample, KIC 6220470, KIC 9474969, and KIC 11071207 (Figure 15), reveal light features around the periastron phase $\varphi_{\rm per}$ (Table 2). The analysis of these observed features led us to the following results:

(a) The observed features around the periastron phase (Figure 15) seem as a 'hump' (brightening). Their shapes differ from the expected ones for the big orbital inclinations (with central dips, see Figures 2–3 of Kumar et al. 1995 and Figure 5 of Thompson et al. 2012).

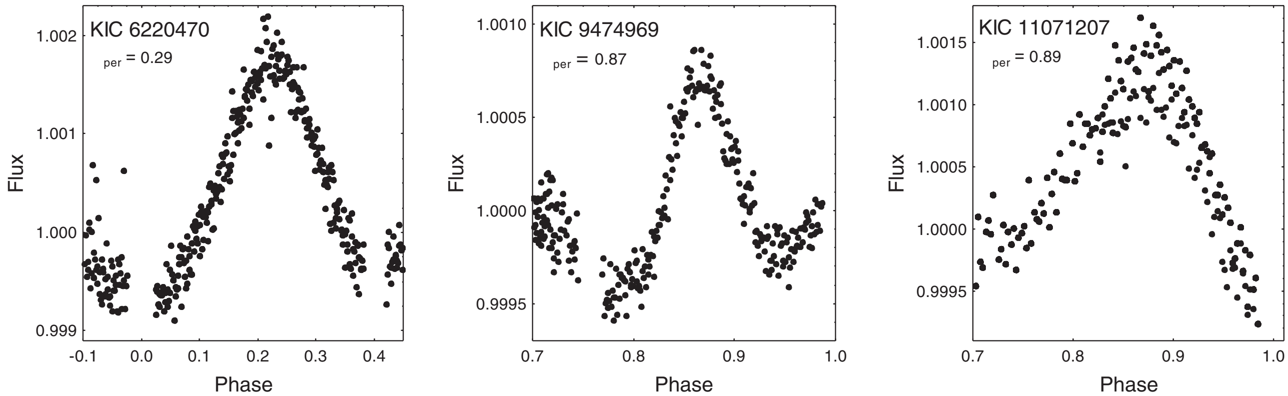

Figure 15. Tidally induced brightening of KIC 6220470 (left panel), KIC 9474969 (middle panel), and KIC 11071207 (right panel).

(b) The hump duration is shortest for KIC 9474969, in which eccentricity is above two times bigger than those of the other two 'humped' targets (see Table 2 and Figure 15). This result supports the conclusion of Thompson et al. (2012).

(c) The tops of the humps do not coincide perfectly with the periastron phases: those of KIC 6220470 and KIC 11071207 slightly precede periastron phase while that of KIC 9474969 slightly delays (Figure 15). These small deviations (phase shifts below 0.04) probably are due to the irradiation effect which phase contribution depends on the periastron angle.

(d) Humps were found only for those targets from our sample for which $r_1 + r_2 \geq 0.09$ (Table 2). This implied that the hump amplitude depends strongly on the relative stellar radii. An additional argument was that the hump amplitude was biggest for KIC 6220470 (Figure 15), in which value $r_1 + r_2 = 0.13$ was the biggest one (Table 3) among the three 'humped' targets of our sample.
To derive the dependence of the hump amplitude on the relative radii, we applied the formalism of Kumar et al. (1995) to eccentric binary consisting of two MS stars and obtained the expression

$$\frac{\delta F}{F} = 4\frac{1}{q}\frac{r_2^3}{(1-e)^3} + 4q\frac{r_1^3}{(1-e)^3}, \qquad (3)$$

where F is the total flux of the target. In fact, this formula gives the amplitude of the 'clean' tidally induced hump. The irradiation effect, in which contribution depends on the periastron angle, superposes the tidally excited brightening and changes the hump amplitude. Moreover, possible tidally-induced pulsations (Willems & Aerts 2002) and Doppler boosting (Bloemen et al. 2011) could cause additional complications.
The hump amplitudes of our targets calculated by expression (1) were around two times bigger than the observed ones. Kumar et al. (1995) obtained just the same discrepancy for PSR 0045-7319. This led us to the supposition about wrong coefficient of their expressions (2 instead of 4).
We should point out that KIC 6949550 has $r_1 + r_2 = 0.1$ but does not reveal a hump. We attributed this exception from the rule (existence of detectable hump for $r_1 + r_2 \geq 0.09$) by its semi-regular variations with bigger amplitude which blur the possible hump.
We assume that the obtained limit of 0.09 of $r_1 + r_2$ depends on the data precision and can be reduced for future space missions.

(e) All targets with periastron brightening have $q \simeq 0.45$. We attributed this fact as a consequence of the accidental coincidence of the binaries with $q \simeq 0.45$ and the systems with biggest relative radii because the dependence (1) of $\delta F/F$ on the relative radii is stronger than that on the mass ratio.

(f) Humps would not be discernable for systems where periastron angle ω is close to 90° or 270° because the periastron phase for these cases will coincide with some of the eclipses. Our targets are not such cases (Table 2), and thus we have not missed some humps for this reason.

(g) We did not find oscillatory modes of any target. This result confirms the conclusion of Kumar et al. (1995) that the MS stars have small amplitudes of oscillation.

6 CONCLUSION

This paper presents the results of determination of the orbits and fundamental parameters of ten EBs with eccentric orbits from the *Kepler* archive. The obtained results allowed us to derive several conclusions.

(1) The formal errors of the derived parameters from the light curve solutions are below 1% (excluding those of KIC 6220470 which exceed 3%).

(2) Our light curve solutions imply that the components of the eccentric binaries (especially those with mass ratios below 0.5) do not follow precisely the empirical relations between the stellar parameters derived from the study of circular-orbit binaries.

(3) KIC 6949550 reveals semi-regular light variations with an amplitude around 0.004 and a period around 7 d which are modulated by long-term variations.
(4) We found tidally induced light ‘hump’ around the periastron phase of three targets: KIC 6220470, KIC 11071207, and KIC 9474969.
(5) We derived formula describing the amplitude of the tidally induced hump of eccentric binary consisting of MS stars. It exhibits that the amplitude of these features increases strongly with the relative stellar radii.
(6) Although we did not find evidences of apsidal motion of our targets in the framework of the relative short duration of the *Kepler* observations, our EEBs present appropriate targets for future study of this effect due to their big eccentricities.

Obviously, the numerous and exclusive precise *Kepler* data deserve precise light curve solutions to enrich statistics of the binaries with estimated parameters and thus to improve the empirical relations between them. Moreover, the tidally induced phenomena provide critical data to constrain the theories of tidal forces in stellar binaries (Fuller & Lai 2011; Burkart et al. 2012).

ACKNOWLEDGEMENTS

The research was supported partly by funds of project RD-08-285 of Scientific Foundation od Shumen University. It used the SIMBAD database and NASA Astrophysics Data System Abstract Service. We worked with the live version of the *Kepler* EB catalogue.

This publication makes use of data products from the 2MASS, which is a joint project of the University of Massachusetts and the Infrared Processing and Analysis Center/California Institute of Technology, funded by the National Aeronautics and Space Administration and the National Science Foundation (Skrutskie et al. 2006). This research makes use of the SIMBAD and Vizier data bases, operated at CDS, Strasbourg, France, and NASA Astrophysics Data System Abstract Service.

The authors are grateful to anonymous referee for the valuable notes and propositions.

REFERENCES

Barembaum, M. J., & Etzel, P. B. 1995, AJ, 109, 2680
Bate, M. 1997, MNRAS, 285, 16
Bate, M., & Bonnell, I. 1997, MNRAS, 285, 33
Bate, M., Bonnell, I., & Bromm, V. 2002, MNRAS, 336, 705
Bloemen, S., et al. 2011, MNRAS, 410, 1787
Bonnell, I., & Bastien, P. 1992, ApJ, 401, 654
Borkovits, T., et al. 2014, MNRAS, 443, 3068
Boyajian, T., et al. 2013, ApJ, 771,
Brown, W. R., Kilic, M., Hermes, J. J., Allende Prieto, C., Kenyon, S. J., & Winget, D. E. 2011, ApJ, 737, L23
Bulut, I., Bulut, A., & Cicek, C. 2014, NewA, 32, 21
Bulut, I., & Demircan, O. 2007, MNRAS, 378, 179
Burkart, J., Quataert, E., Arras, P., & Weinberg, N. N. 2012, MNRAS, 421, 983
Claret, A. 2012, A&A, 541A, 113
Claret, A., & Gimenez, A. 1991, A&A, 244, 319
Claret, A., & Gimenez, A. 1993, A&A, 277, 487
Claret, A., & Gimenez, A. 2010, A&A, 519A, 57
Claret, A., & Bloemen, S. 2011, A&A, 529A, 75
Coughlin, J. L., Lopez-Morales, M., Harrison, T. E., Ule, N., & Hoffman, D. I. 2011, AJ, 141, 78
De Cat, P., Aerts, C., De Ridder, J., Kolenberg, K., Meeus, G., & Decin, L. 2000, A&A, 355, 1015
Dimitrov, D., & Kjurkchieva, D. 2015, MNRAS, 448, 2890
Dimitrov, D., Kjurkchieva, D., & Radeva, V. 2012, BlgAJ, 18c, 81
Duquennoy, A., & Mayor, M. 1991, A&A, 248, 485
Fuller, J., & Lai, D. 2011, MNRAS, 412, 1331
Garcia, E. V., Stassun, K. G., Pavlovski, K., Hensberge, H., Gmez Maqueo Chew, Y., & Claret, A. 2014, AJ, 148, 39
Gimenez, A. 1985, ApJ, 297, 405
Gimenez, A., & Quintana, J. M. 1992, A&A, 260, 227
Graczyk, D. 2003, MNRAS, 342, 1334
Gundlach, C., & Murphy, J. W. 2011, MNRAS, 416, 1284
Hambleton, K. M., et al. 2013, MNRAS, 434, 925
Handler, G., et al. 2002, MNRAS, 333, 262
Harmanec, P., et al. 2014, A&A, 563A, 120
Hernandez-Gomez, A., et al. 2011, RMxAC, 40, 278
Kipping, D. M. 2010, MNRAS, 408, 1758
Kjurkchieva, D., & Dimitrov, D. 2015, AN, 336, 153
Koch, D. G., et al. 2010, ApJ, 713, L79
Kopal, Z. 1978, ASSL (Astrophysics and Space Science Library) 68 (Dordrecht: D. Reidel Publishing Co.)
Kozyreva, V. S., & Kusakin, A. V. 2014, Ap, 57, 221
Kumar, P., Ao, C., & Quataert, E. 1995, ApJ, 449, 294
Kuznetsov, M. V., et al. 2011, ARep, 55, 989
Lacy, C. H. S., Torres, G., Fekel, F. C., Muterspaugh, M. W., & Southworth, J. 2015, AJ, 149, 34
Lajoie, C.-P., & Sills, A. 2011, ApJ, 726, 67
Lehmann, H., Southworth, J., Tkachenko, A., & Pavlovski, K. 2013, A&A, 557A, 79
Levi-Civita, T. 1937, AmJM, 59, 225
Lucy, L. 2006, A&A, 457, 629
Maceroni, C., et al. 2009, A&A, 508, 1375
Maceroni, C., et al. 2014, A&A, 563A, 59
Mathieu, R. D., & Mazeh, T. 1988, ApJ, 326, 256
Michalska, G. 2007, IBVS, no. 5759
Michalska, G., & Pigulski, A. 2004, NewAR, 48, 719
Michalska, G., & Pigulski, A. 2005, A&A, 434, 89
Morris, S. L. 1985, ApJ, 295, 143
North, P., Gauderon, R., Barblan, F., & Royer, F. 2010, A&A, 520A, 74
Petrova, A. V., & Orlov, V. V. 1999, AJ, 117, 587
Pichardo, B., Sparke, L., & Aguilar, L. 2005, MNRAS, 359, 521
Prsa, A., & Zwitter, T. 2005, ApJ, 628, 426
Prsa, A., et al. 2008, ApJ, 687, 542
Prsa, A., et al. 2011, AJ, 141, 83
Sepinsky, J. F., Willems, B., & Kalogera, V. 2007a, ApJ, 660, 1624
Sepinsky, J. F., Willems, B., Kalogera, V., & Rasio, F. A. 2007b, ApJ, 667, 1170
Sepinsky, J. F., Willems, B., Kalogera, V., & Rasio, F. A. 2009, ApJ, 702, 1387
Slawson, R., et al. 2011, AJ, 142, 160
Skrutskie, M. F., et al. 2006, AJ, 131, 1163
Song, H. F., et al. 2013, A&A, 556A, 100
Terrell, D., & Wilson, R. 2005, Ap&SS, 296, 221T
Thompson, S. E., et al. 2012, ApJ, 753, 86

Welsh, W., et al. 2011, ApJS, 197, 4
Willems, B., & Aerts, C. 2002, A&A, 384, 441
Willems, B. 2003, MNRAS, 346, 968
Willems, B., & Claret, A. 2005, SPC, 333, 52W
Willems, B. 2007, ASPC, 361, 124
Wilson, R. E., & Devinney, E. J. 1971, ApJ, 166, 605
Wilson, R. E. 1979, ApJ, 234, 1054
Wilson, R. E., & Van Hamme, W. 2004, Computing Binary Star Observables, in Reference Manual to the Wilson-Devinney Program (Gainesville: University of Florida)
Wilson, R. E., & Van Hamme, W. 2014, ApJ, 780, 151
Wolf, M., Claret, A., Kotkova, L., Kucakova, H., Kocian, R., Brat, L., Svoboda, P., & Smelcer, L. 2010, A&A, 509A, 18
Wolf, M., Zasche, P., Kucakova, H., Lehky, M., Svoboda, P., Smelcer, L., & Zejda, M. 2013, A&A, 549A, 108
Zahn, J.-P. 2005, in ASP Conf. Ser. 333, Tidal Evolution and Oscillations in Binary Stars, ed. A. Claret, A. Gimnez, & J.-P. Zahn (San Francisco: Astron. Soc. Pac.), 4
Zasche, P. 2012, AcA, 62, 97Z
Zasche, P., & Wolf, M. 2013, A&A, 559A, 41
Zasche, P., Wolf, M., Vrastil, J., Liska, J., Skarka, M., & Zejda, M. 2014, A&A, 572A, 71